MULTIFUNCTIONAL COMPOSITE PROCESSED USING EMBROIDERY TECHNOLOGY

Tadashige Ikeda*, Makoto Ishigami, Tsuyoshi Nishihara****
***Chubu University, ****Nagoya University**

Keywords: *embroidery, fiber reinforced plastic, smart structure, optimization, morphing*

Abstract

Multifunctional composites which are composed of resin, reinforcement fibers, and shape memory alloy fibers were proposed. In the composites these fibers were optimally stitched on a base sheet using an embroidery machine so that some objectives were simultaneously satisfied. This stitched dry preform was impregnated with resin by using a vacuum assisted resin transfer molding method. To design an optimal path of the reinforcement fibers, a method to estimate mechanical properties of the stitched reinforcement fiber layer and the base sheet layer having the stitching thread was also proposed. In this paper our R&D activities on such multifunctional composites processed using embroidery technology are introduced.

1 Introduction

Mechanical properties of fiber reinforced plastic (FRP) laminate composites are significantly affected by fiber orientation. If the direction of the loads is different from the fiber by 5 degrees, the longitudinal elastic modulus, E_x, of a carbon fiber reinforced plastic (CFRP) reduces by about 20%, and if the direction is different by 10 degrees, it reduces by about 50% for an example shown in Fig. 1. Accordingly, the FRP composites can be designed more lightly and more sophisticatedly, if the fibers can be placed along a locally curved desired path such as a principal stress direction for example. To this end tailored fiber placement (TFP) methods have been suggested [1-11]. Some researchers [1, 2] use prepreg tows for processing the laminates, while others [3-10] use dry tows, in which the dry tows are placed on a base sheet by using an embroidery machine and impregnated with resin. The former method needs costly prepregs, freezers to store them, and autoclaves suitably-sized for products to harden them, while the latter method does not need such materials and facilities. Accordingly the FRP composites processed by the latter method are expected to be lower-cost.

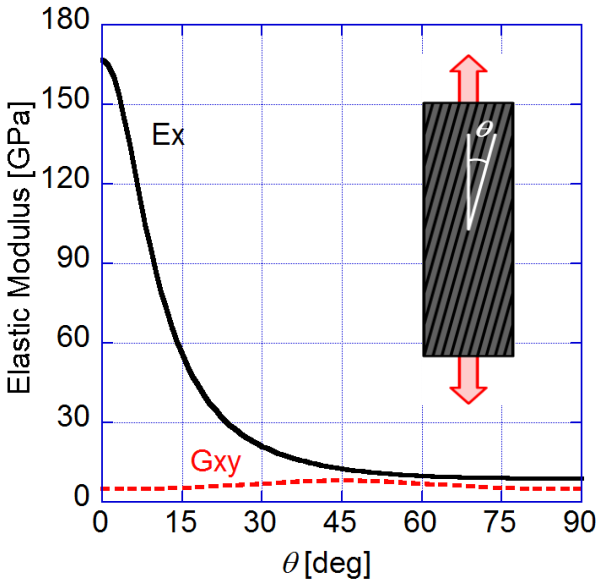

Fig. 1. Variation of Elastic Moduli against the Angle between Fibers and Load Direction.

In our laboratory, Oka et al. [8] proposed a method of design and process for embroidery-based TFP. Figure 2 shows an embroidery machine (Tajima, TCWM-101) used in the study. Carbon fiber bundles were stitched on a base sheet with sewing threads along an optimal path for certain objectives. They verified its availability for a bending-torsion problem of a cantilever plate and also found that effects of the embroidery, such as holes made by a needle

and thickness variation due to the fiber orientation, played important roles on prediction of mechanical properties of the TFP composites. Then Nishida et al. [9] proposed a design method considering such effects to predict the mechanical properties more precisely. Using this method eigen-frequencies of a CFRP cantilever plate were controlled and the error between calculation and experiment was evaluated. To design further light structures Oka et al. [10] proposed a local TFP method where the reinforcement fibers were locally placed. The optimization result of the local TFP showed that it had a comparable performance yet less than a half of weight of the reinforcement fibers for the global TFP. As a next step, we considered that if functional fibers of actuators, sensors, healing agents, and so on could be placed along optimal paths in addition to the reinforcement fibers, the TFP composites could be lighter and smarter as a system and such a smart composite system has a possibility to be a game changer of vehicle and architectural structures. Torii et al. [11] performed an elementary study on creation of new smart multifunctional composites with the reinforcement fibers and the functional fibers whose paths were simultaneously optimized. The multifunctional composite plate composed of Shape Memory Alloy (SMA) fibers as well as reinforcement carbon fibers which were stitched along each curved optimal path so that the displacement at a corner point in a cantilever plate was maximized when the SMA fibers were activated.

In this paper we introduce some of our R&D activities on such multifunctional composites processed by using the embroidery technology. First, in Section 2 the embroidery based TFP and in Section 3 the estimation method of the material constants in each layer of the TFP composites are introduced. SMA fibers are adopted as a functional fiber and a process to combine them with a TFP composite is shown in Section 4. In Section 5 a simultaneous optimization method for the reinforcement fibers and the functional fibers is proposed and a sample of the multifunctional composite is fabricated.

Fig. 2. Embroidery Machine for Tailored Fiber Placement.

2 Embroidery-based TFP

Figure 2 shows the embroidery machine used to place reinforcement fiber bundles on a base sheet. This machine can place the reinforcement fiber bundles in between the base sheet and thread of zigzag stitch sewed along a path input to the machine. The processed dry preform is impregnated with resin by using a vacuum assisted resin transfer molding method (VaRTM). In this study a carbon fiber bundle (Toho Tenax, HTA40-12K) was used as the reinforcement fiber, plain woven carbon fabrics (Toho Tenax, W3101) with a stacking sequence of ($PW45^o/PW0^o$) were used as the base sheet as shown in Fig. 3, and epoxy resin (Sanyu Rec Co. Ltd., ST-7485-A/B) was used as the resin. Top TFP layer is referred to as TFPL, middle 45^o plain woven carbon fabric is referred to as PW_{mid}, and bottom surface 0^o plain woven carbon fabric is referred to as PW_{sur}.

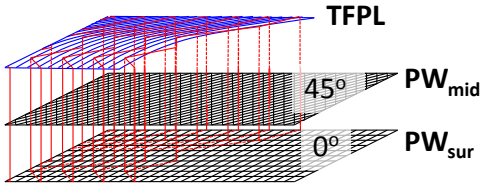

Fig. 3. Schematic Diagram of the Dry Preform with Stacking Sequence of [$TFPL/PW45^o/PW0^o$]. Red lines represent the threads stitching carbon fiber bundles.

3 Estimation of Mechanical Properties of Each Layer [9]

Mechanical properties of the FRP having fiber bundles locally curved stitched by the embroidery machine are affected by not only

fiber orientation and interval between two adjacent fiber bundles but also the threads, the holes opened by a needle, and so on [8,9]. The stacking sequence of the TFP laminate plates considered here was [TFPL/PW45^o /PW0^o]. A pair of square brackets represent the laminates stitched together by the threads. The TFP laminate plates were comprised of TFPL with the threads in the transverse direction and in-plane direction, PW_{mid} with the threads in the transverse direction, and PW_{sur} with the threads in the transverse direction and in-plane direction, as shown in Fig. 3. Accordingly, the structure of each layer is different from each other. The mechanical properties of each layer, in which the effect of the needle and the thread are involved, must be estimated to design the FRP having the TFPL precisely.

In the TFP method adopted in this study, the fiber bundles are placed as shown in Fig. 4. Accordingly, the interval between two adjacent fiber bundles, d, is related to the angle of the fiber bundle, θ, as

$$d=d_0\cos\theta \qquad (1)$$

where d_0 is the interval when the bundles are placed in the 0^o-direction, which is arbitrarily set.

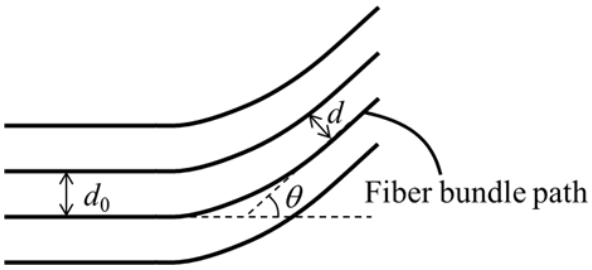

Fig. 4. Variation of Interval between Two Adjacent Fiber Bundle Paths due to Fiber Bundle Angle.

Accordingly, the stiffness matrix and the thickness of the TFPL are given by a function of the fiber bundle orientation θ or the interval d, and they vary during the optimization design process.

To obtain the mechanical properties including the embroidery effects in each layer, FRP plates with stacking sequences of [TFPL0^o/PW45^o/PW0^o]$_S$, [PW0^o/PW0^o], [PW0^o/PW0^o]$_S$, [PW0^o/PW45^o/PW0^o]$_S$, which were stitched with several intervals, were processed and the mechanical properties of the plates were measured by tensile tests. The subscript S represents that a pair of the stitched preforms were symmetrically put together and impregnated with resin. TFPL0^o represents the TFP layer with fiber bundles placed in the 0^o-direction on the base sheet. Regarding the interval, only the interval was varied keeping the fiber bundle angle at 0^o here, although the interval should be related to the fiber bundle angle with Eq. (1) in the practical TFP composite plates. This is because it was assumed that the stitching angle between the direction of the fiber bundles and the base sheet did not affect the mechanical properties of the TFPL and the base sheet layers. The mechanical properties of each layer against the interval were calculated by using the classical laminate theory. In this study, the relationship between resultant forces and in-plane strains becomes

$$\begin{Bmatrix} N_x \\ N_y \\ N_{xy} \end{Bmatrix} = \begin{bmatrix} A_{11} & A_{12} & 0 \\ A_{12} & A_{22} & 0 \\ 0 & 0 & A_{66} \end{bmatrix} \begin{Bmatrix} \varepsilon_x \\ \varepsilon_y \\ \gamma_{xy} \end{Bmatrix} \qquad (2)$$

where

$$A_{ij} = \sum_{k=1}^{N} (Q_{ij})_k t_k$$

$$(Q_{11})_k = \frac{E_{x,k}}{1-\nu_{xy,k}\nu_{yx,k}}$$

$$(Q_{12})_k = \frac{\nu_{yx,k}E_{x,k}}{1-\nu_{xy,k}\nu_{yx,k}} \qquad (3)$$

$$(Q_{22})_k = \frac{E_{y,k}}{1-\nu_{xy,k}\nu_{yx,k}}$$

$$(Q_{66})_k = \frac{1}{\frac{4}{E_{45,k}} - \frac{1}{E_{x,k}} - \frac{1}{E_{y,k}} + \frac{2\nu_{xy,k}}{E_{x,k}}}$$

t, E and ν denote the thickness, Young's modulus, and Poisson ratio, respectively, and the subscripts k, x, y, and 45 represent the material constants in the k-th layer, and those in

the x, y, and 45°-direction, respectively. N, ε, and γ denote the resultant force, in-plane normal strain, and in-plane shearing strain. The specimens $[TFPL0^o/PW45^o/PW0^o]_S$, $[PW0^o/PW0^o]$, $[PW0^o/PW0^o]_S$, $[PW0^o/PW45^o/PW0^o]_S$ are referred to as TFP, PW2, PW4, and PW6, respectively. Here it was assumed that the thickness and the material constants for each corresponding layer were consistent in PW2, PW4, PW6, and TFP. More specifically, it was assumed that PW2 consisted of $(PW_{sur})_S$, PW4 consisted of $(PW_{sur}/PW_{in})_S$, PW6 consisted of $(PW_{sur}/PW_{mid}/PW_{in})_S$, and TFP consisted of $(TFPL0^o/PW_{mid}/PW_{in})_S$. PW_{sur} represents the plain woven layer in the 0°-direction with the threads in the transverse direction and in-plane direction on the surface, and it was distinguished from PW_{in} because PW_{sur} had irregular surface due to the peel ply and the distribution medium for VaRTM. The mechanical properties of PW_{sur} can be obtained from those of PW2, the mechanical properties of PW_{in} can be obtained from those of PW4 and PW_{sur}, the mechanical properties of PW_{mid} can be obtained from those of PW6, PW_{sur}, and PW_{in}, and the mechanical properties of $TFPL0^o$ can be obtained from those of TFP, PW_{in}, and PW_{mid} for each interval between two adjacent fiber bundles.

The tensile tests were carried out with a universal testing machine (Shimadzu, AG-5000B) following JIS K7164. The intervals of the specimens were set to d = 2.0mm, 1.4mm, and 1.0mm, which corresponded to θ = 0°, 45°, and 60°, respectively, when d_0 was set to 2.0mm. Figure 5 shows the elastic moduli and thickness of the TFP plates. Closed symbols, error bars, and lines represent mean, standard deviation, and approximation line, respectively.

The properties for TFP plate could be approximated by liner functions of the interval. The elastic modulus of TFP in the 0°-direction decreases with increase in the interval, while the elastic moduli in the 45° and 90°-direction increase with increase in the interval. The latter is attributed to the fact that the volume fraction of the TFPL decreases but the volume fraction of the fibers in the 45° and 90°-direction increases relatively as the interval increases. The properties for PW2, PW4, and PW6 could be assumed to be independent of the interval.

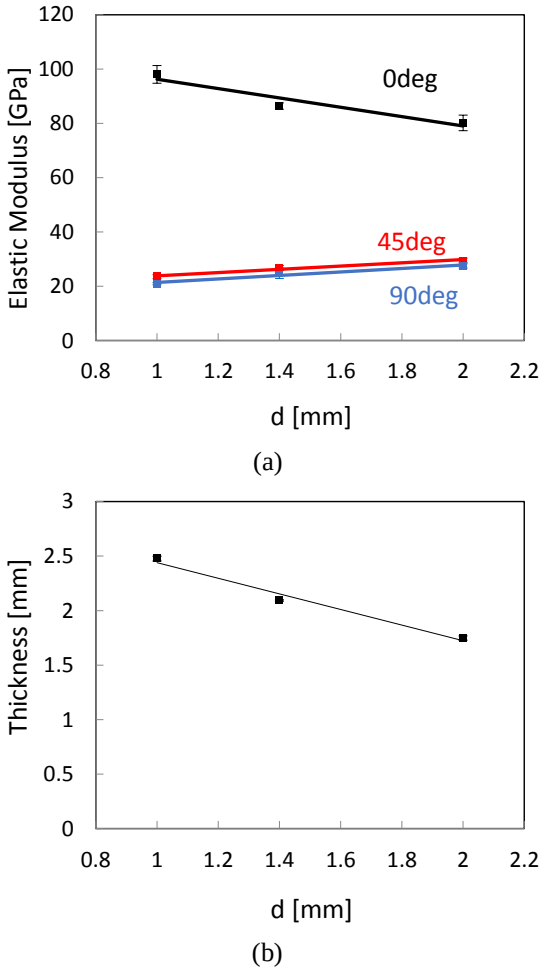

Fig. 5. Elastic Moduli and Thickness of the TFP Plate [11]: (a) Elastic moduli for plate with fibers in 0°, 45°, and 90°-directions, and (b) thickness.

Substituting the obtained approximation values into the classical lamination theory, Eq. (2), the material constants in the longitudinal and transversal direction of the fiber were estimated. They are listed in Table 1. The subscript L and T represent the longitudinal and transverse direction of the fiber, and G denotes the shearing modulus. The material constants of TFPL were assumed to be also a linear function. Here E_L, E_T, and G have become a monotonically increasing function of the interval although those might be a monotonically decreasing function. This may be because the assumption that the thickness and the material constants for PW_{sur}, PW_{mid}, and PW_{in} were consistent in PW2, PW4, PW6, and

TFP was not satisfied, and/or that manufacturing error and measurement error occurred, and so on. However, since $E_L t$, $E_T t$, and Gt were a monotonically decreasing function, here those values were used in the calculation.

Table 1. Estimated Material Constants for Each Layer [11].

	PW_{sur}	PW_{mid}	TFPL(d [mm])
E_L [GPa]	40.4	43.7	27.4d+125.3
E_T [GPa]	40.4	43.7	4.3d+4.6
G_{LT} [GPa]	3.4	4.4	2.0d+2.7
v_{LT}	0.09	0.06	-0.24d+0.80
v_{TL}	0.09	0.06	-0.01d+0.04
t [mm]	0.32	0.30	-0.35d+0.98

4 Functional Fibers

In this study SMA was assumed as a material of functional fibers. SMA fiber varies its length and elastic modulus depending on temperature. Its temperature can be controlled by applying electrical current through the fibers due to Joule heat. To electrically insulate the SMA fibers from the carbon reinforcement fibers, to prevent degradation of the SMA fibers during the hardening process of the resin, and to be able to replace the SMA fibers in case, the SMA fibers were not fixed on the TFP preform directly but a Teflon tube was stitched on the TFP preform by a sewing machine, into which the SMA fibers were assumed to be inserted. Schematic diagram of the Teflon tube with SMA fibers inserted which is stitched on the TFP preform is shown in Fig. 6.

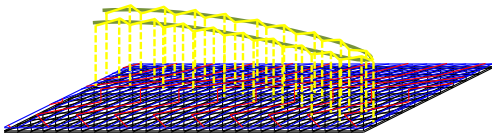

Fig. 6. Schematic Diagram of Teflon Tube with SMA Fibers, Which Is Stitched on a TFP Preform. Yellow lines represent the threads stitching the Teflon tube.

5 An Example of Multifunctional Composites

As an example, consider a multifunctional cantilever plate composed of SMA fibers and TFP plate with a stacking sequence of [TFPL/PW45^o/PW0^o] as shown in Fig. 6. The size of the cantilever plate was 150mm by 100mm as shown in Fig. 7. In this study we would find a simultaneously optimized reinforcement fiber path and SMA fiber path so that the displacement at (x, y) = (145mm, 5mm) was maximized when the SMA fiber shrank by 1% and the averaged deflection of the plate was minimized under uniform pressure of 100Pa. The former is referred to as Objective 1 and the latter as Objective 2.

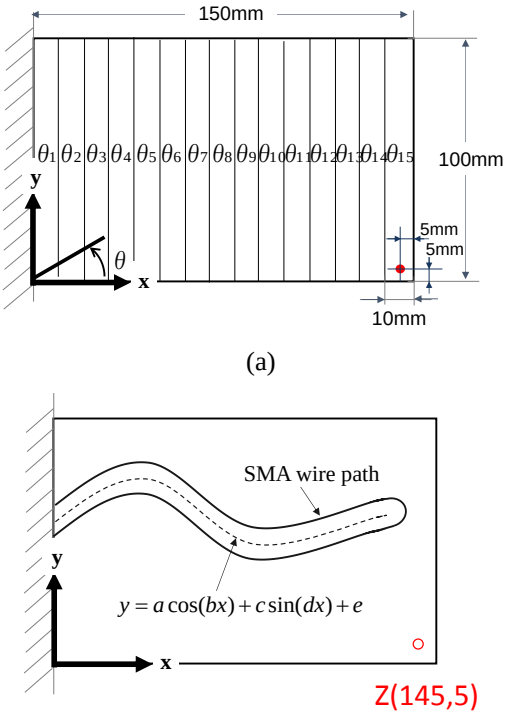

Fig. 7. Definition of the Reinforcement Fiber Angle and an Assumed SMA Fiber Path: (a) Definition of reinforcement fiber angle and measurement point of displacement (red point) and (b) assumed SMA fiber path.

The TFP layer was divided into 15 elements to determine the reinforcement fiber angle and the SMA fiber path was assumed to be U-shaped along a trigonometric function as shown in Fig. 7. This problem is specifically formulated as

Design variables:

$$\boldsymbol{\theta} = [\theta_1, \theta_2, \ldots, \theta_{15}], \quad (4)$$

A = (a, b, c, d, e)

which maximizes:

z_p= z(145, 5) when the SMA fiber shrinks by 1%

and minimizes:

$z_{av}= \sum_{k=1}^{165} z_k /165$ when uniform pressure of 100Pa is acted

subject to constrains:

$-60^o \le \theta_i \le 60^o$ (i=1, 2, …, 15),

$|\theta_{j+1} - \theta_j| \le 30^o$ (j=1, 2, …, 14),

$0 \le a \le 150$, $0 \le b \le 0.05$,

$-50 \le c \le 50$, $0 \le d \le 0.05$,

$10 \le a + e \le 90$

θ = [θ_1, θ_2, …, θ_{15}] denote the reinforcement fiber angle in each element and **A** = (a, b, c, d, e) denote the constants to determine the SMA fiber path. To obtain the averaged displacement, the displacements at 15×11 grid points were averaged, where 15 points were in x-direction and 11 points were in y-direction. The fiber angle was limited within ±60^o and the difference in fiber angle between the adjacent elements was limited within ±30^o. The constants for the SMA fiber path were also limited within certain regions.

Table 2. Material Constants for Functional Fibers Assumed in Calculation.

	SMA	Teflon tube
Elastic modulus [GPa]	12	0.55
Poisson ratio	0.35	0.46
Outer diameter [mm]	0.74	1.60
Inner diameter [mm]	-	0.96

Multi-Objective Genetic Algorithm in Altair HyperWorks14.0 [12] was adopted to find simultaneously optimal paths of the reinforcement fiber bundles and the SMA fiber. The material constants assumed in the calculation for the reinforcement fibers are already listed in Table 1, and those for SMA fiber and Teflon tube are listed in Table 2. In the calculation a single SMA fiber was assumed to be inserted in the Teflon tube for simplicity, although several SMA fibers with a thinner diameter would be assumed to be inserted in practice.

Figure 8 shows a set of optimal solutions. In this problem a single optimal solution cannot be found because trade-offs exist between the two objectives. As can be seen, solutions better for Objective 1 are worse for Objective 2, and vice versa. Values of the objective functions for three typical solutions shown in Fig. 8 are listed in Table 3. In addition, the displacement at (145, 5) of a solution optimized for a single objective function of Objective 1 is also listed, to be referred to as Solution 4. Solution 1 is the best for Objective 2 but the worst for Objective 1 among the three typical solutions shown in Fig. 8 and Solution 3 is the best for Objective 1 but the worst for Objective 2. Solution 4 optimized for only Objective 1 is better than Solution 3 for Objective 1.

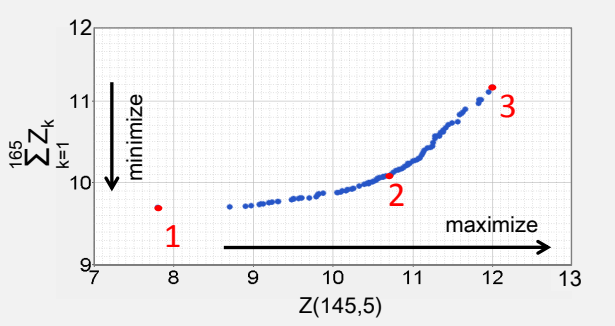

Fig. 8. Set of Optimal Solutions.

Table 3. Values of the Objective Functions for Solutions Shown in Fig. 8 and Solution Optimized for Only Objective 1

	Objective 1 Z(145,5) [mm]	Objective 2 Z_{av} [mm]
Solution 1	7.80	5.88×10^{-2}
Solution 2	10.7	6.11×10^{-2}
Solution 3	12.0	6.77×10^{-2}
Solution 4, optimized for only Objective 1	13.1	-

Figure 9 shows the optimal carbon fiber bundle path and SMA fiber path for Solutions 1, 3, and 4. Both the reinforcement fiber and the SMA fiber paths of Solution 1 have the strongest tendency to be oriented in the 0^o-direction and this structure looks the stiffest for uniform pressure among the three. The SMA

path for Solution 4 has the strongest tendency to be oriented in the principal stress direction when a concentrated load acts at (145, 5) and the reinforcement fiber path has the strongest tendency to become perpendicular to the SMA fiber path. This set of the fiber paths looks good to obtain a large displacement at (145, 5) when the SMA fiber is activated. The reinforcement fiber direction for Solution 3 has is oriented more in the 0^o-direction than Solution 4 and looks better for Objective 2. As can be seen above, the solutions obtained by MOGA are reasonable.

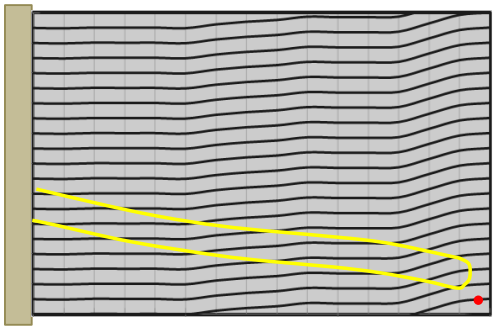

(a)

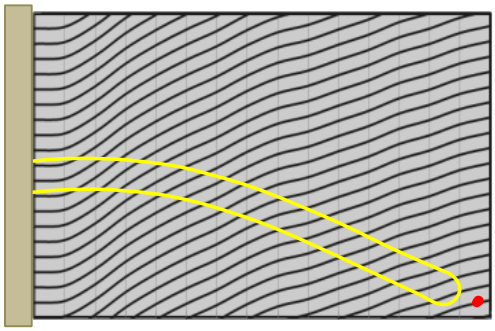

(b)

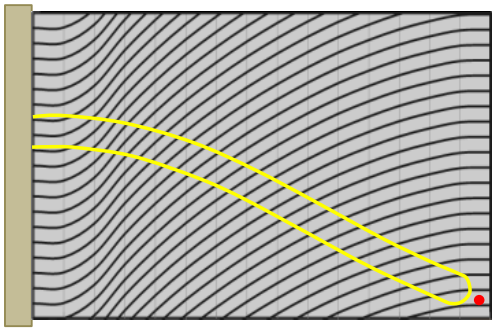

(c)

Fig. 9. Optimal Carbon Fiber Bundle and SMA Fiber Paths for (a) Solution 1, (b) Solution 3 in Fig. 8, and (c) Solution Optimized for Only Objective 1.

To verify the proposed design method practically the multifunctional composite plate for Solution 4 was fabricated as shown in Fig. 10. In this paper two-way SMA fibers (Toki corporation, BMF150, ϕ0.15mm) were inserted into the tube. To activate the SMA fibers an electric current was applied to the SMA fibers and it was confirmed that the plate bent and returned when the power supply was turned on and off, respectively.

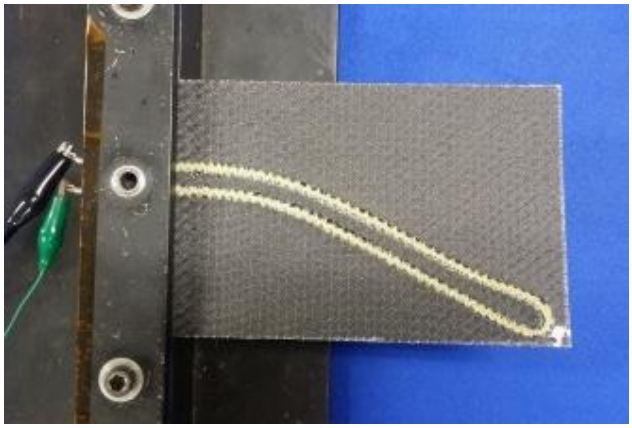

Fig. 10. Fabrication of a Multi-functional Composite Optimized for Only Objective 1 Shown in Fig. 9(c).

6 Conclusions

A multifunctional FRP composite plate composed of SMA fibers and reinforcement carbon fibers was proposed, where these fibers were stitched along optimal curved paths using an embroidery machine. As an elementary problem a set of solutions for simultaneously optimal paths of the SMA fibers and carbon fibers so that a displacement at a certain point of the cantilever plate was maximized when the SMA fibers were activated (Objective 1) and averaged deflection over the plate under uniform pressure was minimized (Objective 2) was found by Multi-Objective Genetic Algorithm. The optimal SMA fiber path tended to be oriented along the direction of the principal stress obtained when a concentrated force acted at the measured point and the reinforcement fiber path tended to be perpendicular to the SMA fiber path for Objective 1 and both the reinforcement fiber and the SMA fiber paths tended to be oriented at

0^{o}-direction for Objective 2. These solutions were made sense. Feasibility of fabrication of the multifunctional composite was also shown practically. Such a smart composite structure is expected to be a game changer of vehicle and architectural structures.

Acknowledgment

A part of this study was supported by JSPS KAKENHI Grant Number 22560781 and 26420811.

References

[1] Tatting, B. F. and Gürdal, Z., "Design and manufacture of elastically tailored tow placed plates," *NASA/CR*, 211919, 2002.

[2] Gürdal, Z. and Tatting, B. F., "Tow-placement technology and fabrication issues for laminated composite structures," *Proc. 46th AIAA/ASME/ASCE/AHS/ASC SDM Conf.*, Austin, USA, AIAA 2005-2017, pp 1-18, 2005.

[3] Crothers, P. J., Drechsler, K., Feltin, D., Herszberg, I. and Kruckenberg, T., "Tailored fiber placement to minimise stress concentrations," *Composites Part A*, Vol. 28A, pp 619-625, 1997.

[4] Mattheij, P., Gliesche, K. and Feltin, D., "3D reinforced stitched carbon/epoxy laminates made by tailored fibre placement," *Composites Part A*, Vol. 31, pp 571-581, 2000.

[5] Temmen, H., Degenhardt, R. and Raible, T., "Tailored fibre placement optimization tool," *Proc. 25th ICAS*, Hamburg, Germany, ICAS2006-4.8.3, pp 1-10, 2006.

[6] Hazra, K., Saverymuthapulle, M., Hawthorne, M., Stewart, D. L., Weaver, P. and Potter, K., "Investigation of mechanical properties of tow steered CFRP panels," *Proc. ICCM17*, D11-5, pp 1-11, 2009.

[7] Panesar, A. S., Hazra, K. and Weaver, P. M., "Investigation of thermally induced bistable behaviour for tow-steered laminates," *Composites Part A*, Vol. 43, pp 926-934, 2012.

[8] Oka, K., Ikeda, T., Senba, A. and Ueda, T., "Design of CFRP with fibers placed by using an embroidery machine," *Proc. ICCM18*, Jeju, Korea, M32-2, pp 1-5, 2011.

[9] Nishida, T., Ikeda, T. and Senba, A., "Optimal fiber placement including effects of embroidery," *Proc. ICCM19*, Montreal, Canada, pp 3865-3872, 2013.

[10] Oka, K., Ikeda, T. and Senba, A., "Optimal placement design of fibers partially set by an embroidery machine," *Proc. APISAT-2013*, Takamatsu, Japan, 07-03-3, pp 1-4, 2013.

[11] Torii, N., Oka, K., and Ikeda, T., “Creation of smart composites using an embroidery machine,” *Proc. SPIE*, Las Vegas, USA, Vol. 9800, 98001C, pp 1-8, 2016.

[12] Altair Engineering, Inc., Altair HyperWorks, viewed 24 June 2018, https://www.altairhyperworks.com/, 2018.

Contact Author Email Address

mailto: ikeda@isc.chubu.ac.jp

Copyright Statement